Received: 19 February 2021 | Revised: 29 June 2021 | Accepted: 19 July 2021

IET Renewable Power Generation

DOI: 10.1049/rpg2.12263

The Institution of Engineering and Technology WILEY

ORIGINAL RESEARCH PAPER

A distributed rule-based power management strategy in a photovoltaic/hybrid energy storage based on an active compensation filtering technique

Seyyed Ali Ghorashi Khalil Abadi | **Ali Bidram**

Department of Electrical & Computer Engineering, University of New Mexico, MSC01 1100, 1 University of New Mexico, Albuquerque, USA

Correspondence
Seyyed Ali Ghorashi Khalil Abadi, Department of Electrical & Computer Engineering, University of New Mexico, MSC01 1100, 1 University of New Mexico, Albuquerque, USA.
Email: ghorashi@unm.edu

Funding information
National Science Foundation New Mexico EPSCoR Program, Grant/Award Number: 1757207

Abstract

This paper proposes a distributed rule-based power management strategy for dynamic power balancing and power smoothing in a photovoltaic (PV)/battery-supercapacitor hybrid energy storage system. The system contains a PV system, a battery-supercapacitor hybrid energy storage system (HESS), and a group of loads. Firstly, an active compensation technique is proposed which improves the efficiency of the power smoothing filter. Then, a distributed supervisory control technique is employed that prevents the BESS and SC from SOC violation while maintaining the balance between generation and load. To this end, the system components are divided into three different reactive agents including an HESS agent, a PV agent, and a load agent. These agents react to the system changes by switching their operational mode upon satisfying a predefined rule. To analyse the hybrid dynamical behaviour of the agents and design the supervisory controllers, the agents are modelled in hybrid automata frameworks. It is shown that the proposed distributed approach reduces the complexity of the supervisory control system and increases its scalability compared to its equivalent centralized method. Finally, the performance of the proposed approach is validated using a test system simulated in MATLAB/Simulink.

1 | INTRODUCTION

The deployment of renewable energy technologies in modern power systems is growing rapidly to reduce the carbon emissions and alleviate global energy crisis by decreasing the dependency on fossil fuels [1]. Photovoltaic (PV) systems use a clean, free, and unlimited source of energy with relatively low maintenance costs. Because of these desirable features, PV systems play an important role in the transformation of the global electricity sector [2]. Photovoltaic systems also enable an economical sustainable solution for remote rural areas in which there is no access to the utility grid [3]. However, balancing the PV's generated power and load is challenging due to the limitation on the availability of power and intermittency of generation. This challenge can be tackled by utilizing energy storage systems (ESSs) as well as implementing effective dynamic power and energy management systems [4, 5].

Among many available ESS devices on the market, battery energy storages systems (e.g., lithium-ion or lead acid batteries) are one of the prevalent energy storages for various applications including residential buildings, renewable energy systems and microgrids. The battery energy storage systems (BESSs) are dispatchable, with low energy losses and relatively low costs. In addition, they have a large energy density that makes them suitable for peak shaving and steady state power balancing. However, the BESSs may have poor performance during sudden load variations or rapid changes of PV power due to their relatively low power capacity and slow dynamic response. In addition, the BESSs have a limited life cycle. Thus, the instantaneous changes of the PV power generation or load power fluctuations may cause frequent charge/discharge of battery that reduces the BESS's lifetime [6, 7] .

The aforementioned limitations of the BESSs can be tackled by effective hybridization of BESSs with supercapacitors (SCs) [8]. SCs have a higher power density and faster dynamic

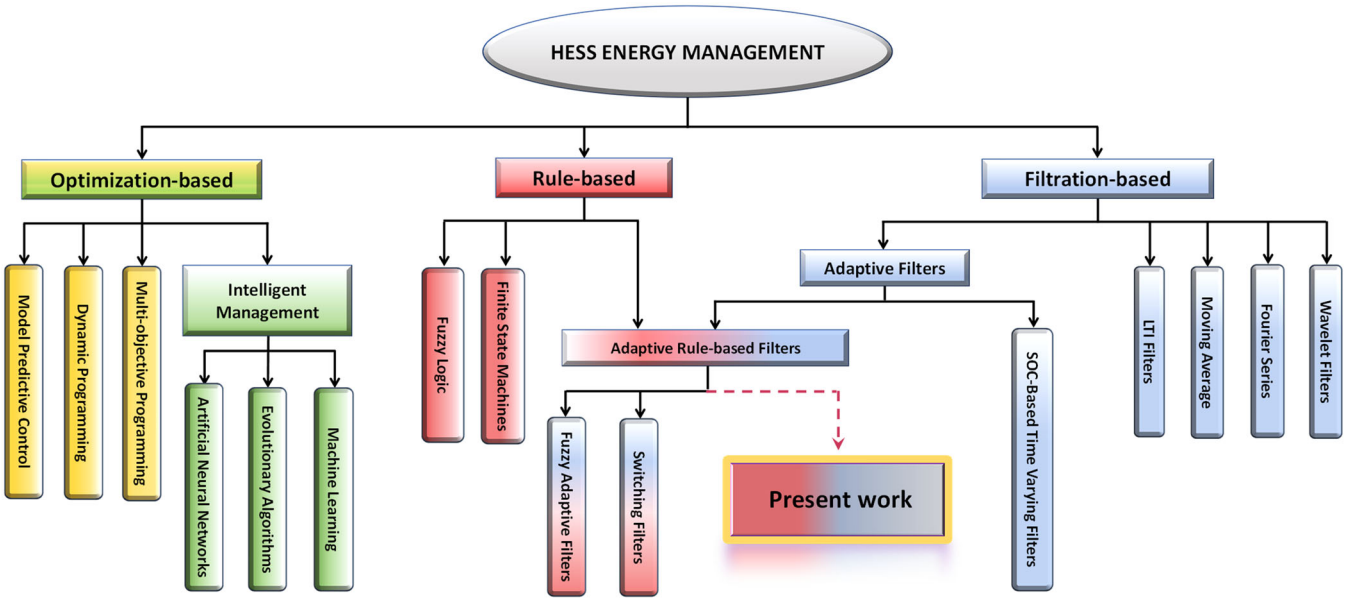

FIGURE 1 Classification of energy management strategies in HESSs with active topologies

response compared to the BESSs which enables them to provide more energy for a considerably shorter time. In addition, they have significantly higher lifecycle than the BESSs. So, the frequent charge/discharge of the SCs does not affect their lifetime [9]. However, the SCs are not suitable for long-term energy storage due to their limited energy density. Considering the underlying limitations and capabilities of the BESSs and SCs, a SC is utilized in tandem with a BESS in battery/supercapacitor hybrid energy storage systems (HESSs) to improve the transient response of the system as well as increasing the life span of the BESSs. To this end, the BESS is utilized for steady state power balancing while the SC absorbs high frequency power fluctuation from the PV and loads [7].

HESSs comprised of BESS and SC may have different topologies including passive, semi-active, and active topologies. Among them, active topologies are superior due to their higher level of controllability. In addition, the energy storage capacity and power dispatch capability of the HESS components (i.e., BESS and SC) can be fully utilized in active topologies. In these topologies, each of the HESS components is individually connected to the system bus through a power electronic converter and has an independent control system. Nevertheless, an efficient control and power management strategy is essential to justify the additional cost of the active components [10].

The effective integration of PV/HESSs depends on optimal sizing as well as appropriate power management and supervision of BESSs and SCs. The optimal sizing of the HESSs can minimize the likelihood of load shedding actions as well as PV power curtailment due to the lack/excess of power generation while considering the cost of components. On the other hand, the power management and supervision techniques aim to perform power allocation of BESS and SC for effective utilization of their storage capacity and operational capabilities as well as ensuring the reliability of the system.

The power management strategies of HESSs can be categorized into optimization-based, filtration-based, and rule-based methods [11]. Figure 1 shows the classification of energy management strategies in HESSs with active topologies. The optimization-based methods can be categorized into model-based and intelligent approaches. The model-based approaches typically include online algorithms (e.g., model predictive controllers) for real time applications or offline algorithms (e.g., multi-objective or dynamic programming) for long-term planning. The intelligent methods also include data-driven approaches such as machine learning-based and artificial neural networks (ANN), or evolutionary algorithms. While these methods can be implemented through both offline and online algorithms, in practice, their high computational complexity may limit their real-time applications [12, 13].

On the other hand, the rule-based methods have lower computational complexity and are more suitable for real-time applications. The rule-based methods can be categorized into finite state machines (FSMs) and fuzzy rule-based approaches. In these methods, the rules can be designed by an expert or based on mathematical models [13].

Due to the simple and powerful structure of FSMs, they are widely used in rule-based dynamic energy management systems for various applications. FSMs or their equivalent finite state automata (FSA) are mathematical models of computation that are widely used in computer science and control for modelling, analysis, and supervisory control of discrete-event dynamic systems. A discrete-event dynamic system (DEDS) is an event-driven system that consists of a set of discrete states and transitions among them. In these systems, the evolution of states (or state transitions) depends on the occurrence of events at discrete instants of time. In FSM-based power management

techniques, each operational mode of the system is associated with a discrete state of an FSA model; the transitions are defined based on the switching rules. The application of FSMs in designing centralized supervisory control and energy management systems has been studied in [14–16]. Furthermore, hybrid automata have been introduced to model and evaluate the interaction between transient response and internal logic of a dynamic rule-based system. To this end, the internal logic and continuous-time dynamics of the system are represented in one frame. This is achieved by labelling continues-time dynamics equations on the discrete state of an FSA. Hybrid automata modelling has been used in [17, 18] to design centralized supervisory control and dynamic energy management systems.

Despite the advantages of FSA techniques to model systems with sequential Boolean logics, they have an intrinsic limitation in modelling concurrent operation of subsystems. In these models, the number of discrete states grows exponentially with the number of processes, which is an obstacle in developing highly flexible and adaptive supervisory control systems [19]. To reduce the complexity, modular modelling techniques can be used to develop an FSA model for each module as well as designing a distributed supervisory control system or use a coordinator agent to manage the appropriate coordination among them [20, 21].

In most microgrid (MG) applications, power management of HESSs is implemented using filtration-based methods [11]. These methods are typically deployed by decomposing the input current (or power) of the HESS into high-frequency and low-frequency components and allocating the high-frequency components into SC. Generally, the implementation of power smoothing filters using linear time invariant (LTI) low-pass filters (LPF) results in less system complexity but lower efficiency. On the other hand, to increase the system efficiency, one can use advanced filtering techniques such as wavelet transformations with the cost of increasing the computational complexity of the charge control system [13, 22].

In practice, using non-ideal filters may result in full charging or discharging of SC. In addition, sudden changes in the input power of the HESS (e.g., a sudden load variation) may impose a considerable stress on the SC module that can immediately fully charge or discharge the SC. To avoid state of charge (SOC) violation of SC and increase the system efficiency adaptive filtering techniques can be applied [5, 23, 24]. In adaptive rule-based filters, typically a rule-based supervisory controller is utilized to relax or deactivate the filter if the SOC of SC violates a certain limit. In this case, more of high frequency components of the HESS input power are sent to BESS to avoid SC SOC violation. Therefore, the size of the SC should be designed appropriately considering the bandwidth of the filter and net power fluctuations. Otherwise, the filter is frequently deactivated that may lessen the system's efficiency. An adaptive SOC-based linear time-varying filter is also presented in [24] for smoothing the output power of wind turbine/HESS. This approach improves the power smoothing capabilities of the HESS by adjusting the time constants of the filters based on SOC variations of the ESSs. However, this technique is basically designed for power smoothing applications, and it is not appropriate for dynamic power balancing purposes.

To address these challenges and improve the efficiency, and reliability, this paper creates a control framework for a PV/HESS system. The case study system contains a group of interconnected loads, a PV power generation system, and a battery-supercapacitor HESS with parallel active topology. The contributions of this paper are as follows:

- An active compensation technique is proposed that improves the efficiency of the power smoothing filter. This approach reduces the minimum required size of the SC for smoothing the input power of the BESS. In addition, it does not increase the computational complexity of the charge control system that makes it suitable for real-time applications.
- Based on the active compensation technique, a hybrid dynamic adaptive filter is designed that ensures reliable operation of the HESS by avoiding SOC violation of SC.
- A distributed supervisory control strategy has been implemented. In this approach, the duties of centralized supervisory controller are distributed among the PV, load, and HESS agent. This technique reduces the computational complexity of the supervisory control system and increase its scalability.
- To analyse the hybrid dynamical behaviour of the agents and design the supervisory control system, the agents are modelled in a standard hybrid dynamical framework (i.e., hybrid automata). This approach facilitates designing a reliable and efficient hybrid supervisory control system for the PV/HESS system.

The rest of the paper is organized as follows: Section 2 introduces the hybrid automata and Section 3 describes the system architecture and components. Section 4 proposes the active compensation technique and presents the designed distributed supervisory control strategy as well as the hybrid automaton model of the agents. The proposed hybrid control strategy is verified through simulation in Section 5. Section 6 discusses the scope and delimitation of this research as well as the future studies. Section 7 concludes the paper.

2 | INTRODUCTION TO HYBRID AUTOMATA

Hybrid automata are standard mathematical frameworks to model, analyse, and design supervisory controllers for hybrid dynamical systems. Hybrid dynamical systems are defined as the systems in which an interaction between continuous-time and discrete-event dynamics exists (e.g., switching systems or reactive agents). In such systems, a discrete event may change the dynamical behaviour of the system. A hybrid automaton with inputs and outputs can be described with a nine-tuple as:

$$\mathcal{H} = \{Q, X, F, E, Inv, U, Y, H, Init\} \quad (1)$$

where Q is a finite set of discrete modes. $X \subseteq \mathbb{R}^m$ is a finite set of real-valued variables associated with the continuous-time states of the system. F denotes a set of vector fields f_{q_i} that represent the evolution of continuous-time dynamics of the system at each discrete mode. Each vector field is a Lipchitz function as $f_{q_i} : X \times U \rightarrow \mathbb{R}^m$. E is the set of all transitions $e_{(i,j)}$. A transition is a four-tuple as $\{q_i, g_{(i,j)}, r_{(i,j)}, q_j\}$ where q_i and q_j are the source and target modes, and $g_{(i,j)}$ is the guard condition. A guard condition is a Boolean expression which is evaluated dynamically based on its associated value. $r_{(i,j)} : \mathbb{R}^m \rightarrow \mathbb{R}^m$ is the reset or update of the transition. The reset maps initialize the dynamics of the system before completing a transition. U is the finite set of inputs and Y is the finite set in which is the set of outputs of the system. H also represents the set of output functions of the system associated with each operational mode and *Inv* is the set of invariants. *Init* is also the set of initial states.

For example, consider a hybrid dynamical system containing two reactive agents (a, b) that have asynchronous mode transitions. Assume that the agent a has three different operational modes (i.e., $Q^a = \{q_1^a, q_2^a, q_3^a\}$) and b has two modes (i.e., $Q^b = \{q_1^b, q_2^b\}$). Consequently, the global system has $n(Q_{ab}) = n(Q_a) \times n(Q_b) = 6$ different operational modes. The dynamical behaviour of these agents changes if they switch to a new operational mode. The dynamics of this system are defined as:

$$\begin{cases} \dot{x}_a = \alpha(q_j^a)x_a + x_b \\ \dot{x}_b = x_a + \beta(q_j^b)x_b + u_c \end{cases} \tag{2}$$

with $\alpha(q_j^a) \in \{-1, -2, -3\}$ and $\beta(q_j^b) \in \{-1, -2\}$. u_c is an external control input and (x_a, x_b) are the continuous time dynamics of agents a and b, respectively.

First, consider that each agent has a supervisory control system that selects the operational mode of that agent, and the agents can communicate with each other (i.e., there is a distributed supervisory control architecture). Figure 2(a) shows a state transition diagram that visually represents the hybrid automata models of the two coordinated reactive agents. Both agents send the value of their continuous state to each other (i.e., $u_a = y_b = x_b$ and $u_b = y_a = x_a$). Agent a is initially in q_1^a operational mode with $x_a(0) = x_0$. In this mode $\alpha(q_1^a) = -1$, so the continuous dynamics of the agent a evolves based on $\dot{x}_a = -x_a + u_a$. Similarly, agent b initially operates in q_1^b operational mode with$x_b(0) = x_0$ and its continuous dynamic evolves as $\dot{x}_b = u_b - x_b + u_c$. Once the state of agent b (i.e., $x_b = u_a$) exceeds a certain value (i.e., $\mathcal{G}_1$) the guard condition $g_{(1,2)}^a$: $u_a > \mathcal{G}_1$ is satisfied and $e^a{}_{(1,2)}$ is activated. So, agent a switches to q_2^a operational mode and changes its dynamical behaviour. In addition, before completing the transition, the initial value of agent a is specified based on the defined reset map (i.e., $r_{(1,2)}^a : x_a(t_0) = x(t^-)$). Similarly, agent b can react to system changes by switching its dynamical behaviour upon stratifying a guard condition.

Alternatively, consider an equivalent system that has a centralized supervisory controller that selects the operational mode of these agents. Figure 2(b) shows the hybrid automaton model

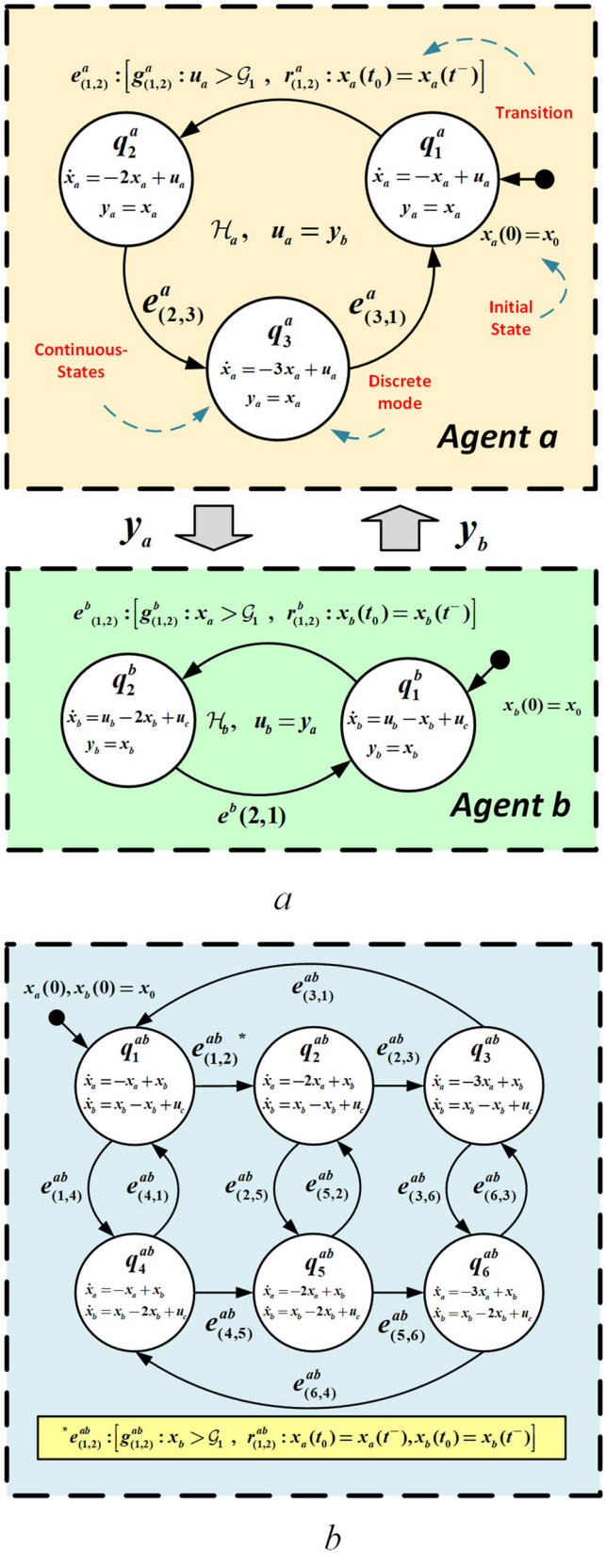

FIGURE 2 State transition diagram of hybrid automata models of two coordinated reactive agents. (a) Distributed supervisory control approach (b) centralized approach (hybrid automata with sequential logic)

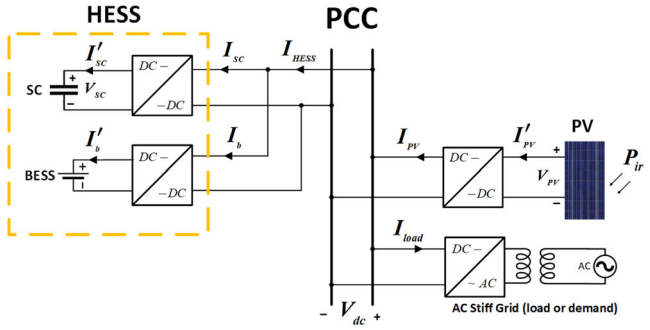

FIGURE 3 The schematic model of the PV/HESS system

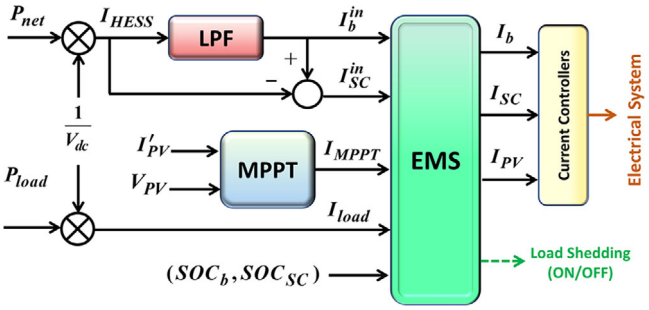

FIGURE 4 The structure of a centralized energy management system in PV/HESSs adopted from [25]

of the global system. To design the equivalent centralized supervisory controller using a hybrid automaton with sequential logic, it is required to define $n(Q_{ab}) = n(Q_a) \times n(Q_b) = 6$ discrete modes and identify the transitions among them. However, in the distributed approach $n(Q_a) + n(Q_b) = 5$ discrete modes are defined.

Now, let assume a system containing N coordinated reactive agents with asynchronous mode transitions that each has M discrete modes. To design a centralized supervisory control system for the global hybrid system using a hybrid automaton with sequential logic, it is required to define M^N discrete modes and identify the transitions among them. Consequently, the complexity of hybrid modelling and supervisory control of the system exponentially increases with the number of agents. However, by utilizing a hybrid automaton framework (with inputs and outputs), the equivalent distributed supervisory control system can be designed by just defining $M \times N$ discrete modes (i.e., M discrete modes for each agent). Thus, the complexity of modelling, and supervisory control of the system can decrease remarkably.

3 | SYSTEM DESCRIPTION

Figure 3 shows the schematic model of the PV/HESS system in this work. The PV module consists of a group of PV panels that are connected to the point of common coupling (PCC) through a DC-DC converter. The HESS module includes a SC and a BESS which are also connected in parallel to the PCC using DC-DC converters (i.e., parallel active topology). The PV/HESS system supplies a group of loads in an AC stiff grid, which is connected to the PCC through an AC-DC converter. The voltage of the PCC is also regulated by the AC-DC converter through connection to the AC stiff grid. So, the HESS module is assumed to operate in current control mode. The AC stiff grid is considered as an AC microgrid that a portion of its power demand is supplied by the PV/HESS system. Knowing the fact that energy management and supervision level has by far slower dynamics, the dynamics of the power electronic converters and low-level controllers (LLC) (e.g., current controllers) are neglected in the rest of this paper.

In HESS power management systems, the net power, i.e.P_{net}, is typically defined as the difference between generated and demanded power. In the case of having a PV system as a single source of generation, the net power can be formulated as:

$$P_{net} = P_{PV} - P_{load} \tag{3}$$

where P_{PV} represents the PV power generation and P_{load} is the demanded power by the load. The net power is used by the HESS to maintain the power balance between the demand and generation. Alternatively, the net power can be written as:

$$P_{net} = P_{HESS} = V_{dc} I_{HESS} = V_{dc}(I_b + I_{SC}) \tag{4}$$

where I_b and I_{SC} are the input currents of BESS and SC from the DC bus side, respectively. V_{dc} is also the voltage of the DC bus.

In practice, the BESSs have limited life cycle. For instance, the estimated life of a lithium-ion battery may vary between 400 to 800 charge cycles. Thus, the instantaneous changes of the net power in a PV power generation system may cause frequent charge/discharge of the battery that reduces the BESS's lifetime. Typically, to increase the BESS lifetime and improve the system efficiency a filtration-based power allocation algorithm is designed that decomposes the net power into high frequency and low frequency components and allocates the high frequency components into SC. Figure 4 shows a conventional centralized energy management system in a PV/HESS for MG applications [11, 25]. In this method, the input reference current of the HESS module (i.e. I_{HESS}) passes from an LPF and then is sent to the current regulator of the BESS. The difference between the HESS and BESS input current ($I_{HESS} - I_b$) is also sent to the SC. Assuming the system is in normal operation (i.e. $I_{SC} = I_{SC}^{in}$, and $I_b = I_b^{in}$) and using an LTI low-pass filter (LPF), I_b and I_{SC} can be obtained as:

$$I_b(s) = G_F(s) I_{HESS}(s) \tag{5}$$

$$I_{SC}(s) = (1 - G_F(s)) I_{HESS}(s) \tag{6}$$

where $G_F(s)$ represents the transfer function of the low-pass LTI filter. Practically, using none-ideal filters and/or severe variations of the net power may result in SOC violation of the SC. To avoid this, the energy management system (EMS) typically deactivates the filter based on predefined rules to avoid SOC violation of the SC module. For example, when the SOC of SC exceeds a certain value, the filter is deactivated and the EMS sends the HESS current to the BESS ($I_b \simeq I_{HESS}, I_{SC} = 0$) to prevent SC from being over charged [23]. Thus, more of the high frequency components of the net power are sent to the BESS in this mode. Consequently, the size of the SC should be designed properly regarding the bandwidth of the filter and the net power fluctuations. Otherwise, the filter is frequently turned off that reduces the system's efficiency.

Moreover, if the SOC of BESS violates its upper limit (i.e. $SOC_b > SOC_{\max}$), the PV power generation should be cut down (i.e. $I_{PV} = I_{load} < I_{MPPT}$) to avoid the BESS's SOC violation. Similarly, if the BESS's SOC reaches to its minimum allowable value, the EMS or supervision system may disconnect unnecessary loads to avoid the instability of MG. It should be mentioned that optimal sizing of the PV/HESS (e.g. long-term planning) or using advanced load and PV power forecasting methods can reduce the likelihood of PV power curtailment as well as load shedding actions that results in more system efficiency. However, to guarantee the reliable operation of the PV/HESS system, it is still necessary to design a real-time supervisory control and energy management system to avoid SOC violation of the BESS and SC.

This paper focuses on improving the performance of the power smoothing filter as well as designing an efficient and reliable real-time energy management and supervision system. To this end, it proposes a hybrid adaptive filtering approach based on the so-called active compensation technique to increase the system efficiency and improve its reliability. To this end, a compensation term will be added to the power smoothing filter that indirectly regulates the SOC of the SC. This technique reduces the SOC variation of the SC that results in reducing the minimum required size of the SC for a same filter bandwidth compared to the conventional method. In addition, a flexible supervisory control system will be designed in a hybrid automaton framework that provides smooth transitions between operational modes of the HESS and ensures the reliability of the PV/HESS system.

4 | PROPOSED CONTROL AND MANAGEMENT SYSTEM

The proposed distributed energy management and supervision system is illustrated in Figure 5. In this structure, every single module of the system (i.e. PV, HESS, and load) has a dedicated energy management system. The coordination among these EMSs forms the global energy management system. Here, PV, load, and HESS can be considered as reactive agents that has have asynchronous mode transitions. The coordination of these agents is as follows:

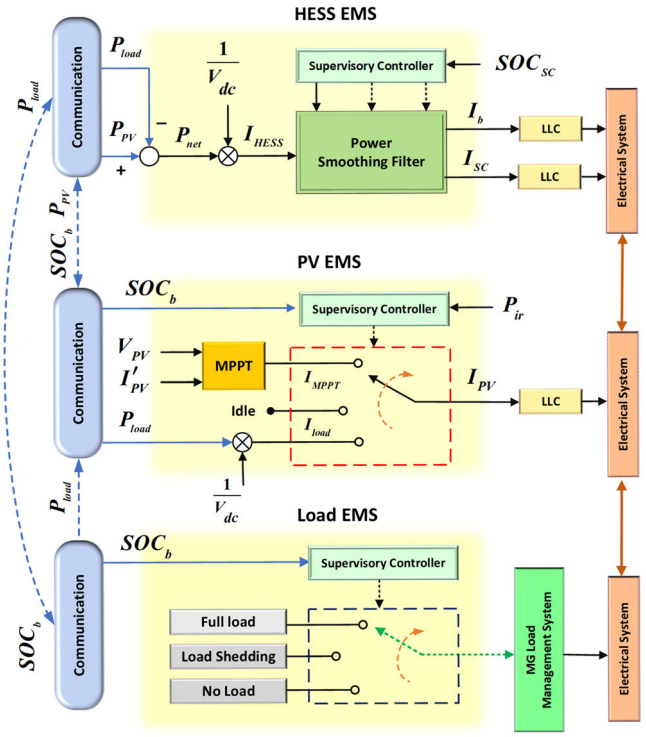

FIGURE 5 The structure of the proposed distributed rule-based power management system

- The HESS agent receives the generation and demanded power (i.e.P_{PV}, P_{load}) from the PV and load agents. P_{PV} and P_{load} is then used by the HESS's EMS to determine the input currents of the BESS and SC (i.e. I_b,I_{SC}). To avoid SC SOC violation, The HESS supervisory controller selects the operational mode of the HESS agent with respect to the SOC of SC.
- The PV agent receives the demanded power (i.e. P_{load}) from the load and SOC value of the BESS (i.e. SOC_b) from the HESS agent. The PV supervisory controller selects the operational mode of the PV with respect to available solar irradiance power (i.e. P_{ir}) and SOC_b to avoid over charging of the BESS as well as ensuring the reliability of the system.
- The load module receives the SOC value of BESS (i.e. SOC_b) from the HESS agent. This value is then used by the load supervisory controller to avoid BESS SOC violation and ensure the stability of the MG.

The following subsections represent the designed control and management system as well as the automaton model of the agents. First, an active compensation filtering technique is proposed that increases the system efficiency without increasing the computational complexity of charge control system. Then, by modelling each agent in a hybrid automaton framework, a distributed supervisory control technique will be applied to ensure the safe and reliable operation of the system.

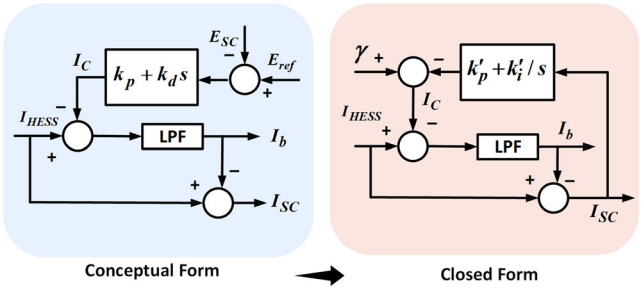

FIGURE 6 The proposed active compensation technique

4.1 | Proposed active compensation technique

4.1.1 | Mathematical formulation and analytical studies

SOC and the stored energy in an SC (i.e. E_{SC}) can be obtained by Equations (7) and (8) as:

$$SOC_{SC}(t) = \frac{1}{Q_n}\int_{t_0} I'_{SC}\,dt + SOC_{SC}(t_0) \tag{7}$$

$$E_{SC}(t) = \frac{1}{2}CV^2_{SC}(t) \tag{8}$$

where V_{SC} and I'_{SC} are the input current and the voltage of the SC from the SC side (see Figure 3). Q_n and C are also the nominal charge and capacitance of the SC. Knowing $I'_{SC} = C\frac{dV_{SC}}{dt}$, and using Equation (7), the SOC of an SC can be represented as:

$$SOC_{SC}(t) = \frac{C}{Q_n}V_{SC}(t) \tag{9}$$

Thus, from Equations (8) and (9) one can obtain:

$$SOC_{SC} \propto \sqrt{E_{SC}} \tag{10}$$

Therefore, by regulating the E_{SC} in a certain range, one can prevent SOC violation in SC. To this end, a compensating term is added to filter that indirectly controls the SOC of the SC. The compensator term is defined as:

$$I_C = k_p(E_{ref} - E_{SC}(t)) - k_d\left(\frac{dE_{SC}}{dt}\right) \tag{11}$$

where k_p and k_d are the proportional and derivative terms of the active compensator and E_{ref} is the reference signal for E_{SC} and it has a constant value (i.e. $\dot{E}_{ref} = 0$). Figure 6 shows the conceptual model of the proposed active compensation technique and its equivalent closed form model. Assuming the filter is linear time invariant (LTI), I_b and I_{SC} are obtained as:

$$I_b(s) = G_F(s)I_{HESS}(s) - G_F(s)I_C(s) \tag{12}$$

$$I_{SC}(s) = (1 - G_F(s))I_{HESS}(s) + G_F(s)I_C(s) \tag{13}$$

where $I_{HESS} = I_b + I_{SC}$ and G_F represents the transfer function of the low-pass LTI filter. Therefore, if $I_C > 0$ the input current of the BESS decreases and that of SC increases to charge the SC with a slight amount of low frequency components. Implementing the proposed filtering technique with the conceptual model in Figure 6 requires the computation of k_p and k_d using a trial-and-error approach as well as measuring E_{SC} which may not be feasible. To avoid this, the discussed approach can be implemented in a closed form as follows. To this end, E_{SC} is defined as:

$$E_{SC} = \int_{t_0} V_{dc}I_{SC}\,dt + E(t_0) \tag{14}$$

Using Equation (14), the compensator term can be represented as:

$$I_C = k_p\left(E_{ref} - \int_{t_0} V_{dc}I_{SC}\,dt - E(t_0)\right) - k_d(V_{dc}I_{SC}) \tag{15}$$

Knowing E_{ref} has a constant value, the compensator term is obtained in the frequency domain as:

$$I_C(s) = -G_C(s)I_{SC}(s) + \frac{k_p\Delta E}{s} \tag{16}$$

where $\Delta E = E_{ref} - E(t_0)$ and $G_C(s)$ is the transfer function of the active compensator which is defined as:

$$G_C(s) = \frac{k'_p s + k'_i}{s} \tag{17}$$

where $k'_i = k_p V_{dc}$ and $k'_p = k_d V_{dc}$. Using Equation (16), Equation (12) can be reformulated as:

$$I_b(s) = G_F(s)I_{HESS}(s) + G_C(s)G_F(s)I_{SC}(s) - k_p G_F(s)\frac{\Delta E}{s} \tag{18}$$

By replacing I_{SC} with $I_{HESS} - I_b$, and $k_p\Delta E = \gamma$, Equation (18) can be represented in a closed form as:

$$I_b = G'_F(s)I_{HESS} - G''_F(s)\frac{\gamma}{s} \tag{19}$$

where $G'_F(s)$ and $G''_F(s)$ are defined as:

$$G'_F(s) = \frac{G_F + G_C G_F}{1 + G_C G_F} \tag{20}$$

$$G''_F(s) = \frac{G_F}{1 + G_C G_F} \tag{21}$$

Similarly, I_{SC} can be represented in a closed form as:

$$I_{SC} = (1 - G'_F(s))I_{HESS} + G''_F(s)\frac{\gamma}{s} \tag{22}$$

Thus, the compensated filter is a multi-input-multi-output (MIMO) LTI filter. Finally, using Equations (19) and (22) the compensated filter is obtained as:

$$\begin{bmatrix} I_b(s) \\ I_{SC}(s) \end{bmatrix} = \begin{bmatrix} G'_F(s) & -G''_F(s) \\ 1 - G'_F(s) & G''_F(s) \end{bmatrix} \begin{bmatrix} I_{HESS}(s) \\ \frac{\gamma}{s} \end{bmatrix} \tag{23}$$

Using Equations (7) to (10), γ can be also defined as:

$$\gamma = \rho(SOC_{ref}{}^2 - SOC_{SC}{}^2(t_0)) \tag{24}$$

where ρ is the charging coefficient defined as $\rho = (k'_i Q_n^2)/(2V_{dc}C)$. Equation (24) shows that γ is a function of the reference SOC (i.e. SOC_{ref}) as well as the initial SOC value of the SC. This definition facilitates regulating the SOC of SC when its initial value is different from the reference SOC.

It should be mentioned that to model the system in a hybrid automaton framework and design the supervisory controller, it is required to define the dynamics of the compensated filter in the state space form. Here, assume that the original LPF is a second order LTI filter defined as:

$$G_F = \frac{1}{(\alpha s + 1)^2} \tag{25}$$

where α is the filter coefficient. Using Equations (20) and (21), the transfer functions of the filter with using active compensation technique is obtained as:

$$G'_F = \frac{(1 + k'_p)s + k'_i}{\alpha^2 s^3 + 2\alpha s^2 + (1 + k'_p)s + k'_i} \tag{26}$$

$$G''_F = \frac{s}{\alpha^2 s^3 + 2\alpha s^2 + (1 + k'_p)s + k'_i} \tag{27}$$

Using Equations (23), (26), and (27), the dynamics of the compensated filter can be represented in the state space form as:

$$\begin{cases} \dot{x}_F(t) = A_F x_F(t) + B_F u_F(t) \\ y_F(t) = C_F x_F(t) + D_F u_F(t) \end{cases} \tag{28}$$

where $x_F = [x_1, x_2, x_3]^T$, $u_F(t) = [I_{HESS}, \gamma]$, and $y_F(t) = [I_b, I_{SC}]^T$. A_F, B_F, C_F, and D_F are also obtained as:

$$A_F = \begin{bmatrix} 0 & 0 & -k'_i/\alpha^2 \\ 1 & 0 & -(1 + k'_p)/\alpha^2 \\ 0 & 1 & -2/\alpha \end{bmatrix} \tag{29}$$

$$B_F = \begin{bmatrix} k'_i/\alpha^2 & (1 + k'_p)/\alpha^2 & 0 \\ 0 & -1/\alpha^2 & 0 \end{bmatrix}^T \tag{30}$$

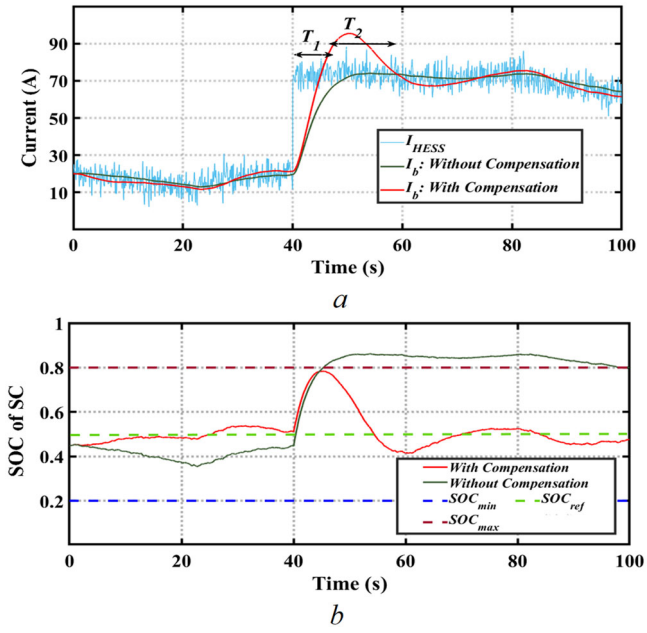

FIGURE 7 The performance of the proposed compensation technique ($I_{SC} = I_{HESS} - I_b$). (a) Input current of the HESS and battery (b) SOC variation of the SC

$$C_F = \begin{bmatrix} 0 & 0 & 1 \\ 0 & 0 & -1 \end{bmatrix} \tag{31}$$

$$D_F = \begin{bmatrix} 0 & 0 \\ 1 & 0 \end{bmatrix} \tag{32}$$

The dynamical equation of the compensated filter represented in Equations (28) to (32) will be used later in Section 4.1.2 to analyse the performance of the proposed active compensation technique and in Section 4.2.1 to design the hybrid supervisory controller of the HESS module. In addition, these equations show that the proposed active compensation technique does not require any additional information or measurements and it does not increase the computational complexity of the charge control system making it suitable for real-time applications. While this method can be utilized for both non-linear and linear filters, in the case of using an LTI filter, the closed form formulation enables the system designer to select the parameters of the filter in an analytical manner considering the dynamic stability and the bandwidth of the filter.

4.1.2 | Empirical analysis

Considering Equations (29) to (32), the performance of the proposed active compensation technique is illustrated in Figure 7. The case study system is a SC with 4 s charge time and 30 kW nominal power and $V_{dc} = 300$V. The BESS also has 30 kW nominal power and 2 h charge time. The filter parameters are $\alpha = 2$, $k'_i = 0.12$, $k'_p = 0.003$, $SOC_{ref} = 0.5$, and the initial SOC of SC is 0.45 (i.e. $SOC_{SC}(t_0) = 0.45$). As seen, by

defining γ using Equation (24), the compensated filter smoothly charges the SC to increase its SOC to the reference value (i.e. $SOC_{ref} = 0.5$) after around 15 s. On the other hand, without compensation technique the SOC of SC does not reach to the desired point (i.e. $SOC_{ref} = 0.5$). At $t = 40$ s, a sudden load change happens. This load change imposes a high stress on the HESS that charges the SC with $I_{SC} = I_{HESS} - I_b$ during a short time interval represented by T_1 (see Figure 7(a)). The load change results in SOC violation of the SC when there is no active compensation. However, the active compensation technique generates an overshoot current during T_2 interval that discharges SC to prevent its SOC violation and regulates its SOC to the reference value. Thus, the proposed active compensation technique lessens the SOC variation of the SC that reduces the minimum required size of SC and increases the system efficiency. It should be noted that the proposed technique can have similar impact on the other types of linear and non-linear filters.

4.2 | Supervisory controllers

In the proposed rule-based approach, the supervisory control system is designed to avoid SOC violation of the HESS components (i.e. BESS and SC) while maintaining the balance between generation and load. To reduce the computational complexity and improve the scalability, the tasks of a centralized supervisory control system are distributed among the PV, load, and HESS agent. To this end, the HESS supervisory controller is responsible for the efficient and reliable operation of HESS as well as avoiding SOC violation of the SC. On the other hand, avoiding BESS SOC violation is dedicated to the PV and load supervisory controllers. In addition, the cooperation between supervisory controllers ensures the balance between generation and load in all operating modes. In what follows, the supervisory controller of each agent and its hybrid automaton model will be discussed.

4.2.1 | HESS agent

To avoid SC SOC violation, a hybrid adaptive filtering technique is utilized in the HESS module. The filter is compensated using the proposed technique in Section 4.1. Figure 8 shows the structure of the proposed hybrid adaptive filtering technique. In this approach, if the SOC of SC exceeds a certain value, the bandwidth of the filter increases to lessen the stress on the SC. To this end, the HESS supervisory controller changes the dynamics of the filter by adjusting the filter parameters (i.e. α,k'_p, andk'_i). In addition, it updates the value of γ and specifies the initial states of the filter (i.e. $x_F(t_0)$) before switching to the new operational mode for regulating the SOC of the SC as well as ensuring the stability of the system after switching instances.

Figure 9 represents the state transition diagram of the hybrid automaton model of the HESS agent where$x_F = [x_1, x_2, x_3]^T$ is the continuous dynamics of the filter and $u_F = [I_{HESS}, \gamma]^T$

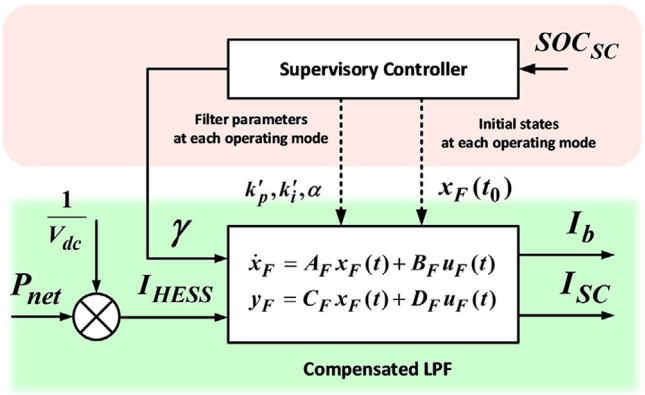

FIGURE 8 The proposed hybrid adaptive filtering technique

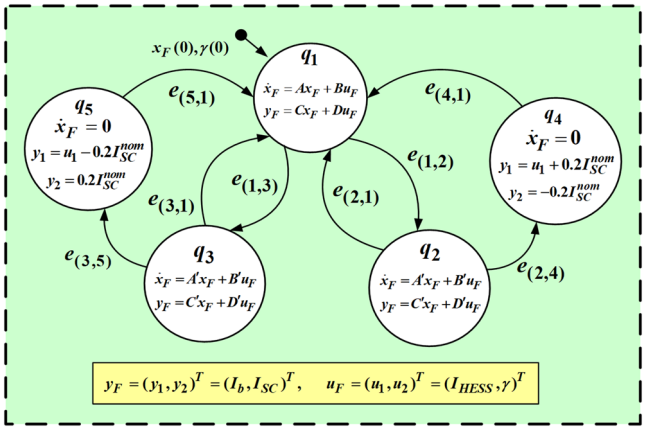

FIGURE 9 State transition diagram of the hybrid automaton model of the HESS agent

represents the inputs (see Equation (28)). This hybrid automaton model shows the interaction between continuous-time dynamics and discrete logic of the HESS agent.

To balance the power generation and load I_{HESS} is defined as:

$$I_{HESS} = P_{net}/V_{dc} = (P_{PV} - P_{load})/V_{dc} \tag{33}$$

where P_{PV} is the photovoltaic power generation and P_{load} is the load power. The state space parameters of the dynamical model of the compensated filter in q_1 and q_2 or q_3 operational modes are respectively defined as:

$$\{A, B, C, D\} = \{A_F, B_F, C_F, D_F\}|_{k'_p=\ell_2, k'_i=\ell_1, \alpha=\ell_0} \tag{34}$$

$$\{A', B', C', D'\} = \{A_F, B_F, C_F, D_F\}|_{k'_p=\ell'_2, k'_i=\ell'_1, \alpha=\ell'_0} \tag{35}$$

whereA_F, B_F, C_F, and D_F are defined in Equations (29)–(32). $\{\ell_0, \ell_1, \ell_2\}$ also represent the filter parameters in q_1 operating mode and $\{\ell'_0, \ell'_1, \ell'_2\}$ are the filter parameters in $q_2$and q_3 modes. In Figure 9, $e_{(i,j)} = \{q_i, g_{(i,j)}, r_{(i,j)}, q_j\}$ represents a transition from operational mode q_i to q_j . Table 1 shows the guard

TABLE 1 Guard conditions of the HESS agents

Guard	Expression	Guard	Expression
$g_{(1,2)}$	$SOC_{SC} > 0.7$	$g_{(1,3)}$	$SOC_{SC} < 0.3$
$g_{(2,1)}$	$SOC_{SC} \leq 0.5$	$g_{(2,4)}$	$SOC_{SC} > 0.8$
$g_{(3,1)}$	$SOC_{SC} \geq 0.5$	$g_{(3,5)}$	$SOC_{SC} < 0.2$
$g_{(4,1)}$	$SOC_{SC} \leq 0.5$	$g_{(5,1)}$	$SOC_{SC} \geq 0.5$

TABLE 2 Characteristics of the tested filters

Test cases	Filters	Characteristics		
		Adjusting α, k'_p, k'_i	Resetting γ	Resetting $x_F(t_0)$
Case 1	Filter1	Off	Off	Off
	Filter2	On	Off	On
	Filter3	On	On	On
Case 2	Filter1	On	On	Off
	Filter2	On	On	On

conditions (i.e. $g_{(i,j)}$) of the supervisory controller. q_1 represents the normal operation of the HESS agent. Based on the discrete logic of the HESS illustrated in Figure 9, the agent switches to q_2 or q_3 operational modes when $g_{(1,2)}$ or $g_{(1,3)}$ are satisfied. (i.e. $SOC_{SC} > 0.7$ or $SOC_{SC} < 0.3$). In these modes, the supervisory controller changes the dynamics of the filter and increases the filter bandwidth to reduce the stress on the SC module. If this mode changing is not effective enough to control the SOC of SC, the agent will switch to the SC recovery modes represented by $q_4$andq_5 to protect the HESS's devices. In these modes, the supervisory controller deactivates the filter and SC is smoothly charged or discharged by 20% of its nominal power. Once the SOC of SC reaches to a predefined value, the filter switches back to the normal operation.

In hybrid dynamical systems, the switching resets (or initialization) have a significant impact on the transient response and stability of the system after switching instances [26]. In the proposed hybrid filtering method, any transient current oscillation after switching instances can affect the performance of the power smoothing filter by charging or discharging the SC. In one hand, after switching to q_2 operating mode (i.e. $SOC_{SC} > 0.7$), to discharge the SC and return to normal operating mode (i.e. $SOC_{SC} \leq 0.5$), it is required to send a negative transient current to SC. Similarly, after switching to q_3 mode, it is necessary to send a positive transient current to SC, to charge it and switch back to q_1. On the other hand, when the HESS switches back to normal operation a bump less transition (i.e. transition with no current fluctuation) is needed to maintain the SOC of SC to the reference value.

Assume a hybrid system that has a stable equilibrium at each mode. If the initial states of this system in each discrete mode are equal to their steady state value (i.e. equilibrium point) the system will not experience any transient oscillation after switching instances. Using Equations (29) to (32), the steady state values of the filter dynamics (i.e. $x_F^* = [x_1^*, x_2^*, x_3^*]^T$) in $q_j \in \{q_1, q_2, q_3\}$ operating mode can be obtained as:

$$\dot{x}_F^* = 0 \rightarrow x_1^* = \frac{\gamma}{\alpha_j^2}, x_2^* = \frac{2}{\alpha_j} I_{HESS}^*, x_3^* = I_{HESS}^* \tag{36}$$

where α_j is the filter coefficient in q_j mode defined in Equations (29) to (32). Consequently, by properly defining the reset maps, one can manage the transient current oscillations to regulate the SOC of SC and ensure the reliable operation of HESS after switching instances. To this end, using Equations (24) and (36), the reset maps (i.e. $r(i,j), j \in \{1,2,3\}$) are defined as:

$$r_{(i,j)} = \{x_1(t_0) = 0, x_2(t_0) = \frac{2}{\alpha_j} x_3(t^-), x_3(t_0) = x_3(t^-), \\ \gamma(t_0) = \rho_j({SOC_{ref}}^2 - {SOC_{SC}}^2(t^-))\} \tag{37}$$

where t^- is the time when the transition is activated and t_0 is the time at which the transition is completed. α_j and ρ_j are also the value of filter coefficient and charging coefficient (see Equations (24)–(29)) at the new operational mode (i.e. q_j). With this definition, when the system switches back to normal operation (i.e. q_1), γ is updated to zero (i.e. $\gamma(t_0) = 0$). So, the initial states of the filter become equal to their steady state value (i.e. $x_F(t_0) \neq x_F^*$) and the HESS experiences a bump less transition to q_1. On the other hand, if the system switches to q_2 or q_3, γ will be updated to a negative or positive value, respectively. Consequently, $x_F(t_0) \neq x_F^*$ and the charge control system generates a transient current fluctuation that discharges/charges the SC and regulates its SOC to the reference value (i.e. SOC_{ref}). It should be mentioned that in SC recovery modes (i.e. q_4, q_5) the filter is deactivated, so the initial states do not have any impact on the outputs of the filter. Thus, $r(i,j), j \in \{4,5\}$ are not specified.

The impact of the switching resets on SOC regulation of the SC as well as system's stability has been studied in two test cases. Table 2 represents the characteristics of the filters used in these test cases. In both cases, the study system is like the study system of the example in Section 4.1.2.

Case 1 highlights the performance of the proposed hybrid adaptive filtering technique as well as the necessity of resetting γ after mode transitions. Figure 10 illustrates the performance of the three tested filters in this test case with $SOC_{SC}(0) = 0.52$ and $SOC_{ref} = 0.5$. All the filters initially have a small negative value for γ (i.e. $\gamma(0^+) \simeq -1.6$) to slightly discharge the SC and regulate its SOC to the reference value. Then, a sudden load change happens at $t = 40$ s. As seen, Filter 1 is not able to respond to the load change and fails to maintain the SOC of the SC within the allowable range (i.e. $0.2 < SOC_{SC} < 0.8$). On the other hand, in Filter 2 and Filter 3, once the SOC of SC exceeds 0.7 (at $t^- = 41.7$ s), the supervisory controller increases the bandwidth of the filter by switching to the q_2 operational mode at $t_0 = 41.7^+$s. Consequently, the SOC of the SC remains in the allowable range for both filters. However, in Filter 2, γ

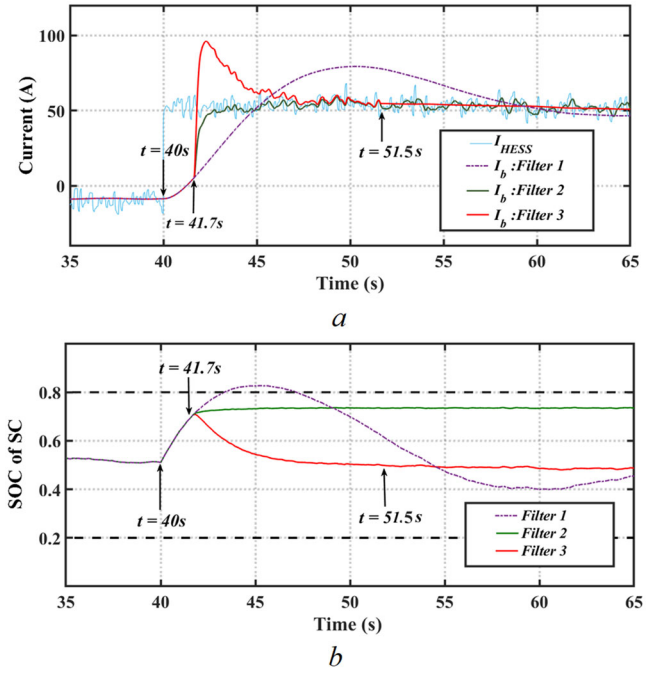

FIGURE 10 The performance of the filters in Case 1. ($\ell_0 = 2, \ell_1 = 0.2, \ell_2 = 0.01, \ell'_0 = 0.1, \ell'_1 = 0.5, \ell'_2 = 0.005$) (a) Input current of the HESS and battery (b) SOC variation of the SC

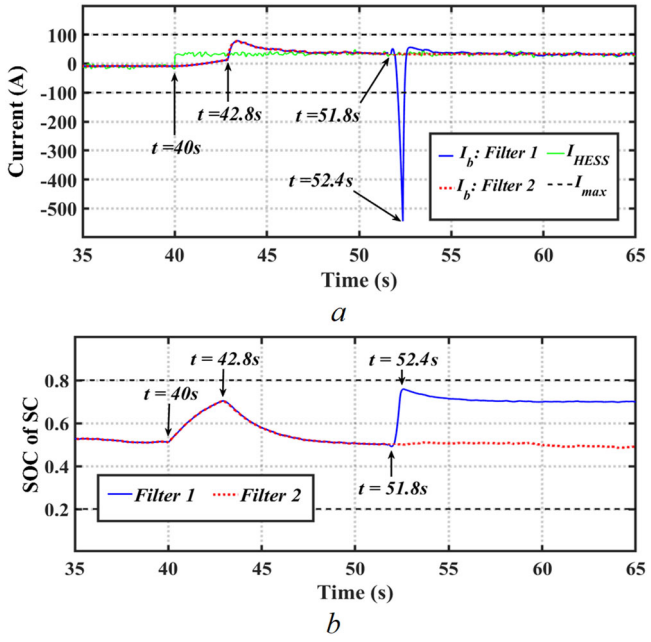

FIGURE 11 The performance of the filters in Case 2. ($\ell_0 = 2, \ell_1 = 0.2, \ell_2 = 0.01$ $\ell'_0 = 0.1, \ell'_1 = 0.5, \ell'_2 = 0.005$) (a) Input current of the HESS and battery (b) SOC variation of the SC

is not updated (i.e. $\gamma(41.7^-) = \gamma(41.7^+) \simeq -1.6$) and the SOC of SC remains equal to 0.7. So, the HESS agent is locked in q_2 operational mode and it cannot switch back to normal operation. On the other hand, Filter 3 discharges SC by updating γ to a larger negative value when it switches to q_2 (i.e. $\gamma(41.7^-) \simeq -1.6, \gamma(41.7^+) \simeq -48$). Thus, it regulates the SOC of SC to the reference value and switches back to q_1 at $t_0 = 51.5^+$s. In addition, at $t_0 = 51.5^+$s, Filter 3 pushes γ to zero (i.e. $\gamma(51.5^+) = 0$) to ensure a bump less transition to q_1. Similarly, if the system switches toq_3, γ will be updated to a positive value that results in charging the SC. Here, resetting γ to a positive/negative value is like intentionally generating an overshoot current (see Figure 10(a)) that charges/discharges the SC to regulate its SOC to the reference value. It should be noted that in all the operating modes the input current of the SC is equal to difference between HESS and BESS current (i.e. $I_{SC} = I_{HESS} - I_b$). So, this overshoot current does not have any impact on the power balancing performance of the system and Equation (33) is always satisfied.

Case 2 highlights the necessity of precisely resetting the initial states (i.e. $x_F(t_0)$) to avoid unintentional transient current oscillations after switching instances. In this test case, the first HESS agent employs a typical gain scheduling adaptive filter (i.e. Filter 1). This filter maintains its previous states as the initial values for the new operational mode (i.e. $x_F(t_0) = x_F(t^-)$). On the other hand, the second agent is designed based on the proposed hybrid adaptive approach (i.e. Filter 2) and it resets the initial values using Equation (37) before completing the transitions. The performance of the two tested filters is illustrated in Figure 11.

In this test case a sudden load change happens at $t = 40$ s. Consequently, to avoid SOC violation, both filters switch to $q_2$operational mode at $t_0 = 42.8^+$s and increase their bandwidth. In addition, both HESS agents update γ before completing the transition (i.e. $\gamma(42.8^+) \simeq -48$) to regulate the SOC of the SC to the reference value (i.e.$SOC_{ref} = 0.5$ Then, the guard condition $g_{(1,2)}$ is satisfied at $t^- = 51.8$ s and both HESSs switch to the normal operation and update γ (i.e. $\gamma(51.8^+) \simeq 0$). However, the first HESS that uses Filter 1 experiences a significant uncontrolled current fluctuation after switching back to normal operation (i.e. q_1). This current fluctuation is beyond the nominal value of the BESS current, and it may damage or destabilize the system. In addition, it charges SC again and the HESS switches back to the q_2 at $t_0 = 52.4^+$s to avoid SC SOC violation. Consequently, this agent cannot switch back to the normal operation to smooth the input current of the BESS. However, by defining the switching resets as Equation (37) one can eliminate the uncontrolled current fluctuation after switching instances.

In conclusion, if the SOC of SC violates a certain range (i.e. $SOC_{SC} > 0.7$ or $SOC_{SC} < 0.3$), the HESS agent switches to q_1 or q_3 operational modes. Once the agent switches to these modes, the charge control system generates a controlled transient current to regulate the SOC of SC to the reference value (i.e. $SOC_{ref} = 0.5$). Then, once the SOC of SC reaches to its reference value, the HESS switches back to q_1 operational mode. Then, the HESS experiences a bump less transition (i.e. transition with no current oscillation) to maintain the SOC of SC to the reference value. The proposed supervisory control approach is achieved by modelling and analysing the system behaviour in a standard hybrid dynamical framework (i.e. a hybrid

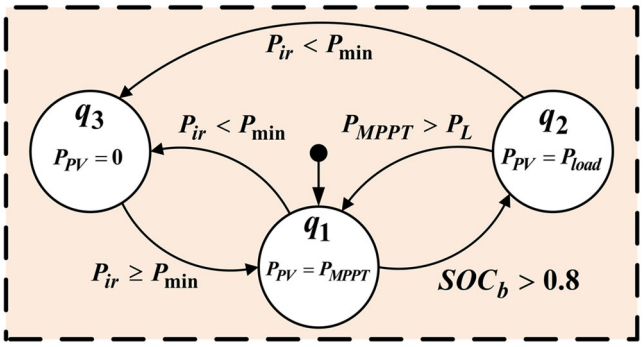

FIGURE 12 State transition diagram of the automaton model of the PV module

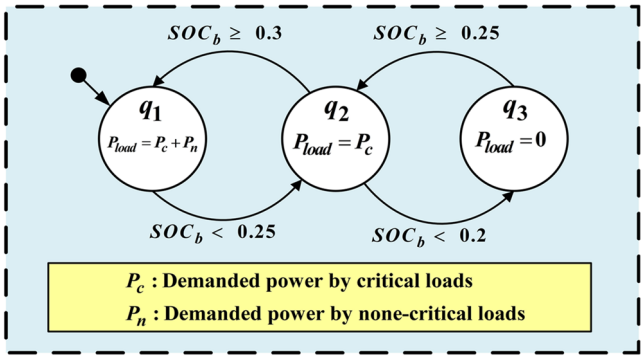

FIGURE 13 State transition diagram of the automaton model of the load agent

automaton) as well as properly defining the guard conditions and reset maps.

4.2.2 | PV and load agents

The PV and load energy management systems are designed with respects to the following operational constraints:

- The SOC of BESS must vary within a predefined range (i.e. $0.2 < SOC_b < 0.8$). Otherwise, the BESS will be damaged.
- The PV/HESS system must always deliver the demanded power by load to the upstream grid (i.e. AC MG). So, any imbalance between the PV power generation and load is stored/supplied by the HESS.
- The loads, in the upstream grid, are classified into critical (i.e.P_c) and non-critical loads (i.e. P_n). During the normal operation of the system, the PV/HESS supplies the total demanded power by the critical and non-critical loads (i.e. $P_{load} = P_c + P_n$).
- To avoid discharging of the BESS as well as maintaining the balance between generation and load, the load management system can disconnect a portion of the loads. Knowing the fact that the critical loads have higher priority, the non-critical load are disconnected first in load shedding actions.
- To avoid overcharging of the BESS while maintaining the balance between the generation and load, the PV power generation must be cut down if the SOC of the BESS reaches to its maximum allowable value. Otherwise, the BESS will be damaged or there will be an imbalance between the generation and load.
- The PV system should be disconnected if the available solar irradiance power is lower than a threshold value (i.e. $P_{ir} < P_{\min}$).

Considering the above operational constraints, a rule-based EMS is designed for each of the load and PV agent. The logic of the PV agent is represented by an automaton illustrated in Figure 12. The PV agent has three operational modes, including maximum power point tracking (MPPT), load following, and idle modes. The system is initially in MPPT mode (i.e. q_1 and $P_{PV} = P_{MPPT}$). If the SOC of BESS reaches to its maximum value (i.e. $SOC_b > 0.8$), to avoid overcharging of the battery, PV reduces its power generation and switches to the load following mode (i.e. $P_{PV} = P_{load} < P_{MPPT}$). In addition, if the available solar irradiance power is less than the threshold value (i.e. $P_{ir} < P_{\min}$) the PV switches to the idle mode.

Figure 13 shows the automaton model of the load module. This agent has three operational modes including full load, load shedding, and system recovery modes. When the SOC of BESS decreases from a saturation value (i.e. $SOC_b < 0.25$), the load module switches to the load shedding operational mode by disconnecting the non-critical loads. If this load shedding action is not sufficient to increase the SOC of BESS, the system will be forced to switch to the recovery mode by disconnecting all the loads. This action is necessary to maintain the stability of system and protect the system's devices. The load module switches back to the full load mode if the SOC of BESS exceeds 0.3 (i.e. $SOC_b \geq 0.3$).

Knowing that load shedding or PV power curtailment is costly, optimal sizing of the PV/HESS is necessary to lessen the likelihood of load shedding actions and PV power reduction. In general, optimal sizing of the PV/HESS requires long-term planning which is out of scope of this paper. Here, it is assumed that the PV/HESS is efficiently sized. So, the PV power curtailment or load shedding actions would be infrequent during the long-term operation of the system.

In this paper, PV, load, and HESS agents have asynchronous mode transitions. As discussed in Section 2, utilizing a distributed approach for designing the supervisory control system can reduce the computational complexity compared to an equivalent centralized structure. In the proposed distributed supervisory control approach the HESS agent has five operational modes. PV and load modules also have three operational modes. Thus, the total number of discrete modes is equal to the summation of the operational modes, i.e. eleven. On the other hand, to design an equivalent centralized supervisory controller using the hybrid automata with sequential logic, it is required to define 5×7 discrete modes and identify the transitions among them that can be a tedious task. In addition, any change (e.g. adding new devices) to the system requires a significant reconfiguration of the centralized controller. Therefore, the proposed

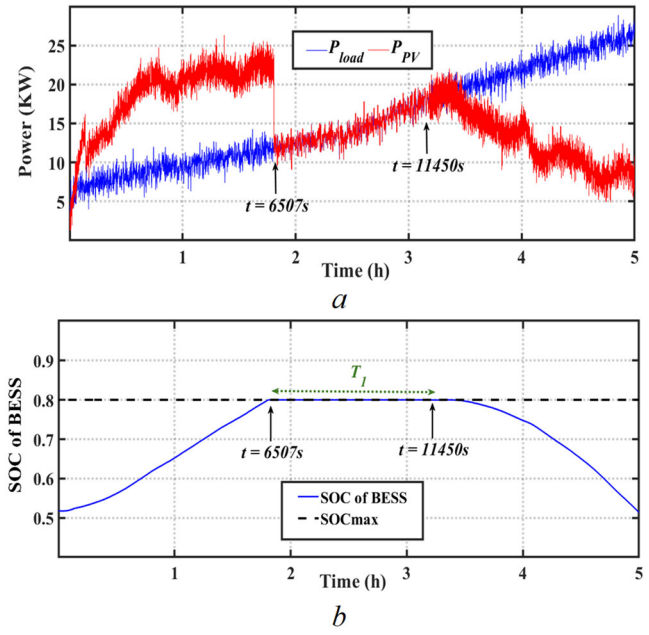

FIGURE 14 Power sharing and battery SOC balancing performance of the PV/HESS system. (a) Generation and load power (b) SOC of BESS

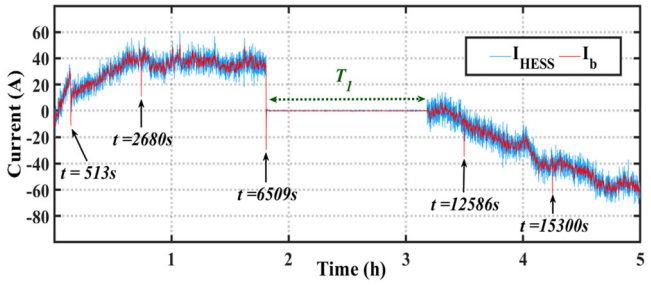

FIGURE 15 Input current of the HESS module

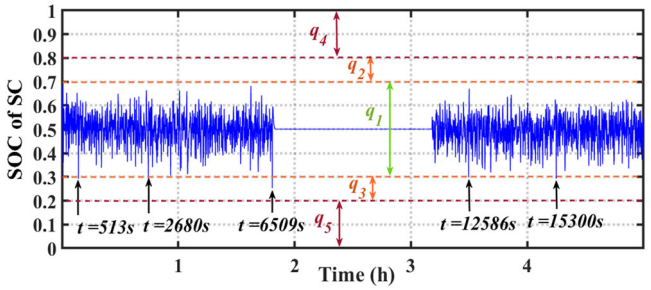

FIGURE 16 SOC variation of SC (proposed approach).q_i is the associated region with each operational mode of the HESS

distributed strategy reduces the computational complexity of the supervisory control system and increases its scalability.

5 | SIMULATION RESULTS

This section analyses the performance of proposed distributed rule-based supervisory control and power management system in mid-term operation of the system using MATLAB/Simulink. To this end, an unplanned situation has been simulated in which the BESS can be overcharged due to the excess of PV power generation. The BESS nominal power and energy is 30 kW/60 kWh. The SC has also 30 kW nominal power and 4 s of charge time. The PV and load module have 30 kW nominal power and the voltage of PCC, V_{dc}, is equal to 300 V. The filter parameters are defined based on Equations (34) and (35) as $\ell_0 = 4, \ell_1 = 0.04, \ell_2 = 0.004, \ell'_0 = 0.5, \ell'_1 = 0.5$, and$\ell'_2 = 0.05$.

5.1 | Power balancing and power smoothing performance of the proposed technique

Figure 14 represents the battery SOC control and power balancing performance of the system. Initially, the PV module is in the MPPT mode and BESS's SOC is 0.52 (i.e. $SOC_b(0) = 0.52$). Then, the SOC of BESS reaches to its maximum allowable value (i.e. $SOC_{\max} = 0.8$) at $t = 6507$ s. At this time, the guard condition $g_{(1,2)} : SOC_b \geq 0.8$ is satisfied (see Figure 12) and the PV agent switches to the load following mode (i.e. $P_{PV} \simeq P_{load} < P_{MPPT}$). Consequently, the net power becomes zero (i.e. $P_{net} = P_{PV} - P_{load} \simeq 0$) and the SOC of BESS remains the same value. During this time (i.e. $t \in T_1$), the available solar power gradually decreases while that of load demand increases. At $t = 11450$ s, the demanded power becomes more than the maximum power generation of the PV module (i.e. $P_{load} > P_{MPPT}$). So, the PV switches to the MPPT mode and the BESS releases power to maintain the balance between generation and load.

Figure 15 illustrates the input current of the HESS module (i.e. I_{HESS} and I_b). The power smoothing filter charges/discharges the BESS with low-frequency components of the net power. As seen, when the PV is in load following mode (i.e. $t \in T_1$), the input current of the HESS is approximately zero.

The SOC variation of the SC module of the HESS is illustrated in Figure 16. As seen, when the PV switches to the load following mode at $t = 6507$ s the input current of the HESS suddenly changes. As a result, the SC is discharged at $t = 6509$ s and the guard condition $g_{(1,3)} : SOC_{SC} < 0.3$ is satisfied. So, the system switches to the q_3 mode to avoid SC SOC violation. Similarly, there are four additional switching instances (i.e. $t = 513$ s, $t = 2680$ s, $t = 12,586$ s, and $t = 15,300$ s) in which the HESS switches to the q_3 operating mode to avoid SC SOC violation. Consequently, the SOC of SC always remains in the allowable range during the simulation interval. Before switching to q_3, the BESS generates an overshoot current (see Figure 10(a)) to regulate the SOC of SC to the reference value (i.e. $SOC_{ref} = 0.5$). These generated overshoot currents at switching instances are annotated in Figure 16. It should be noted that the input current of SC is always equal to difference between HESS and BESS currents (i.e. $I_{SC} = I_{HESS} - I_b$), consequently, the SC absorbs these transient currents which satisfies Equation (33). In another word, charging or discharging the SC by

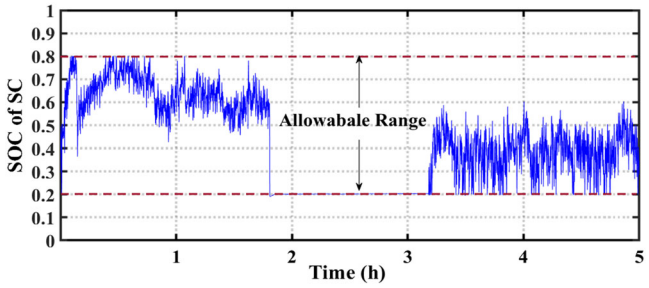

FIGURE 17 SOC variation of SC in the conventional rule-based method proposed in [25]

TABLE 3 Comparative analysis

	Power management strategy	
Factors	**Proposed approach**	**Conventional approach in [25]**
NSI	5	96
SBCV	274	301

the BESS does not affect the power balancing performance of the PV/HESS system.

5.2 | Comparative analysis

This section compares the performance of the proposed technique with a conventional rule-based power management system presented in [25]. To this end, the performances of both power management techniques are compared considering the two following factors.

- Number of Switching Instances (NSI),
- Sum of the BESS Current Variation (SBCV).

NSI value represents the number of instances that the filter is deactivated/relaxed to avoid SC SOC violation. Knowing the fact that switching instances may cause some small transient oscillations on the DC bus voltage, the lower NSI value represents a better performance for the system. SBCV is also defined as:

$$SBCV = \sum_{k=K_0}^{K} |I_b(kT_s) - I_b(kT_s - T_s)| \tag{38}$$

where $T_s = 30\text{ms}$ is the sampling time and $t = [K_0 T_s, KT_s]$ is the simulation interval. Thus, the lower BESS current variation results in lower SBCV that shows a better power smoothing performance of the system. Figure 17 shows the SC SOC variation of the conventional rule-based approach for the test case scenario defined in Section 5.1.

A comparison between these two approaches has been provided in Table 3. In the conventional rule-based technique, there is no active compensation which results in higher SOC variation for the same size of the SC compared to the proposed approach (see Figure 17). Consequently, the power smoothing filter is frequently deactivated to avoid SC SOC violation. In this case, the number of switching instances during the simulation interval (i.e. NSI value) is 96. However, the NSI value for the proposed approach is 5. In addition, by frequently deactivating the filter (i.e. $I_b = I_{HESS}$, $I_{SC} = 0$) more of high frequency components of the HESS current are allocated to the BESS that results in higher SBCV value for the conventional rule-based approach. In this case, the SBCV value is 301 while SBCV value is 274 for the proposed approach. Thus, the proposed approach significantly reduces the number of switching instance (i.e. NSI value) and slightly lessens (i.e. by around 9%) the SBCV value that highlights the better performance of the proposed power management technique.

6 | DISCUSSION

This research mainly focuses on improving the performance and the efficiency of the power smoothing filter as well as reducing the computational complexity of the energy management system. So, without loss of generality, a relatively simple model for the PV and load module is considered. However, because of the scalability and distributed architecture of the proposed approach, one can easily add more details (e.g. more operational constraints) to the PV and load models without changing or adjusting the logic or continuous-time dynamics of the HESS agent.

Moreover, it is assumed that the HESS operates as a grid following unit. Then, knowing that the power management system has by far slower dynamics, the dynamics of low-level controllers and power electronic converters are neglected. Compared to the conventional rule-based methods, the proposed approach adjusts the bandwidth of the filter to avoid SC SOC violation instead of fully deactivating the filter. The authors believe that this feature may have additional advantages such as improving the dynamic stability and transient response of the system compared to conventional methods if the HESS operates as a grid forming unit in an islanded DC MG. Thus, the future research direction will be on developing a detailed dynamic model of the system to investigate the impact of this technique on the dynamic stability of an islanded DC MG if the HESS operates as a grid forming unit.

7 | CONCLUSION

In this paper, a distributed rule-based supervisory control and power management technique in a PV/HESS system is presented. The case study system consists of a PV, a load, and a HESS that contains a BESS and a SC. Each module is an intelligent agent that can react to the environment by changing its dynamical behaviour and/or operational mode. First, an active compensation filtering technique is proposed that improves the system's efficiency by controlling the SOC variation of the SC. Then, to design the distributed supervisory control system, the

hybrid automaton modelling approach is employed. The proposed hybrid modelling framework facilitates designing a hybrid adaptive filter for the HESS agent that can manage the current oscillations after switching instances. The distributed supervisory control approach provides efficient the reliable operation of PV/HESS system by preventing the SCs and BESSs from SOC violation. In addition, the proposed distributed power management technique reduces the computational complexity of the supervisory control system compared to its equivalent centralized method. Finally, the performance of the proposed rule-based power management strategy is verified by simulating the PV/HESS system in MATLAB/Simulink.

ACKNOWLEDGMENTS

This paper is based upon work supported by the National Science Foundation New Mexico EPSCoR Program under Award #OIA- 1757207.

Nomenclature

C	Capacitance of the SC
E_{SC}	Stored energy in SC
I_b	BESS input current from the DC bus side
I_C	Compensation current
I_{HESS}	HESS input current
I_{load}	Load input current from the DC bus side
I_{PV}	PV output current from DC bus side
I_{SC}	SC input current from the DC bus side
I'_b	BESS input current from the battery side
I'_{PV}	PV output current from the PV panel side
I'_{SC}	SC input current from the SC side
k_d	Derivative gain of the active compensator in the conceptual model.
k_p	Proportional gain of the active compensator in the conceptual model.
k'_i	Integral gain of the active compensator
k'_p	Proportional gain of the active compensator in closed form model
P_c	Demanded power by critical loads
P_{HESS}	HESS power
P_{ir}	Available solar irradiance power
P_{load}	Load power demand
P_n	Demanded power by non-critical loads
P_{net}	Net power
$P_{\min}$	Threshold value for PV power generation
P_{PV}	Photovoltaic power generation
Q_n	Nominal charge capacity of the SC
SOC_b	State of charge of the battery
SOC_{ref}	Reference state of charge of the SC
SOC_{SC}	State of charge of the SC
V_{dc}	Voltage of the DC bus
V_{PV}	Terminal voltage of the PV panels
V_{SC}	SC's terminal voltage
α	Filter coefficient
ρ	Charging coefficient of the SC
BESS	Battery energy storage system
EMS	Energy management system
ESS	Energy storage system
FSA	Finite state automata
FSM	Finite state machines
HESS	Hybrid energy storage
LLC	Low-level controllers
LPF	Low-pass filter
MG	Microgrid
NSI	Number of switching instances
SBCV	Sum of BESS current variation
SC	Supercapacitor
SOC	State of charge

ORCID

Seyyed Ali Ghorashi Khalil Abadi https://orcid.org/0000-0001-7965-0185
Ali Bidram https://orcid.org/0000-0003-4722-4346

REFERENCES

1. Khodadoost Arani, A.A.B., Gharehpetian, G., Abedi, M.: Review on energy storage systems control methods in microgrids. Int. J. Electr. Power Energy Syst. 107, 745–757 (2019)
2. Cristaldi, L., et al.: Model-based maximum power point tracking for photovoltaic panels: Parameters identification and training database collection. IET Renewable Power Gener. 14(15), 2876–2884 (2020)
3. Jha, S., et al.: Optimal operation of PV-DG-battery based microgrid with power quality conditioner. IET Renewable Power Gener. 13(3), 418–426 (2019)
4. Tummuru, N.R., et al.: Control strategy for AC-DC microgrid with hybrid energy storage under different operating modes. Int. J. Electr. Power Energy Syst. 104, 807–816 (2019)
5. Zhang, Y., Du, G., Lei, Y.: Energy management strategy with two degrees of freedom for hybrid energy storage systems in islanded DC microgrids. IET Power Electron. 13(14), 3188–3198 (2020)
6. Li, S., et al.: Adaptive energy management for hybrid power system considering fuel economy and battery longevity. Energy Convers. Manage. 235, 114004 (2021)
7. Jing, W., et al.: Battery-supercapacitor hybrid energy storage system in standalone DC microgrids: Areview. Inst. Eng. Technol. 11, 461–469 (2017)
8. Wang, Y., et al.: A review of key issues for control and management in battery and ultra-capacitor hybrid energy storage systems. eTransportation 4, 100064 (2020)
9. Şahin, M.E., Blaabjerg, F.: A hybrid PV-battery/supercapacitor system and a basic active power control proposal in MATLAB/simulink. Electron 9(1), 129 (2020)
10. Jing, W., et al.: Dynamic power allocation of battery-supercapacitor hybrid energy storage for standalone PV microgrid applications. Sustainable Energy Technol. Assess. 22, 55–64 (2017)
11. Hajiaghasi, S., Salemnia, A., Hamzeh, M.: Hybrid energy storage system for microgrids applications: A review. J. Energy Storage 21, 543–570 (2019)
12. Lin, P., et al.: A semi-consensus strategy toward multi-functional hybrid energy storage system in DC microgrids. IEEE Trans. Energy Convers. 35(1), 336–346 (2020)
13. Bocklisch, T.: Hybrid energy storage systems for renewable energy applications. Energy Procedia 73, 103–111 (2015)
14. Wang, Y., Sun, Z., Chen, Z.: Energy management strategy for battery/supercapacitor/fuel cell hybrid source vehicles based on finite state machine. Appl. Energy 254, 113707 (2019)
15. Trigkas, D., et al.: Supervisory control of energy distribution at autonomous RES-powered smart-grids using a finite state machine approach. In: 2018 5th International Conference on Control, Decision and Information Technologies, CoDIT 2018. Thessaloniki, Greece, pp. 415–420 (2018)
16. Khawaja, Y., et al.: An integrated framework for sizing and energy management of hybrid energy systems using finite automata. Appl. Energy 250, 257–272 (2019)

17. Liu, J., Chen, Y.: An online energy management strategy of parallel plug-in hybrid electric buses based on a hybrid vehicle-road model. In: IEEE Conference on Intelligent Transportation Systems, Proceedings, ITSC. Rio de Janeiro, pp. 927–932 (2016)
18. Kafetzis, A., et al.: Energy management strategies based on hybrid automata for islanded microgrids with renewable sources, batteries and hydrogen. Renewable Sustainable Energy Rev. 134, 110118 (2020)
19. Zhao, J., et al.: Modeling and control of discrete event systems using finite state machines with variables and their applications in power grids. Syst. Control Lett. 61(1), 212–222 (2012)
20. Sugumar, G., et al.: Supervisory energy-management systems for microgrids: Modeling and formal verification. IEEE Ind. Electron. Mag. 13(1), 26–37 (2019)
21. Dou, C., et al.: Event-triggered hybrid control strategy based on hybrid automata and decision tree for microgrid. IET Gener. Transm. Distrib. 13(14), 3066–3077 (2019)
22. Guo, T., et al.: A dynamic wavelet-based robust wind power smoothing approach using hybrid energy storage system. Int. J. Electr. Power Energy Syst. 116, 105579 (2020)
23. Zhang, X.-Z., et al.: Fuzzy adaptive filtering-based energy management for hybrid energy storage system. Comput. Syst. Sci. Eng. 36(1), 117–130 (2021)
24. Nguyen, V.T., Shim, J.W.: Virtual capacity of hybrid energy storage systems using adaptive state of charge range control for smoothing renewable intermittency. IEEE Access 8, 126951–126964 (2020)
25. Singh, P., Lather, J.S.: Power management and control of a grid-independent DC microgrid with hybrid energy storage system. Sustainable Energy Technol. Assess. 43, 100924 (2021)
26. Paxman, J.: Switching Controllers: Realization, Initialization and Stability. University of Cambridge (2003)

How to cite this article: Ghorashi Khalil Abadi, S.A., Bidram, A.: A distributed rule-based power management strategy in a photovoltaic/hybrid energy storage based on an active compensation filtering technique. IET Renew. Power Gener. 1–16 (2021)
https://doi.org/10.1049/rpg2.12263